Content-aware Directed Propagation Network with Pixel Adaptive Kernel Attention

Min-Cheol Sagong, Yoon-Jae Yeo, Seung-Won Jung, Senior Member, IEEE, and Sung-Jea Ko, Fellow, IEEE

Abstract-Convolutional neural networks (CNNs) have been not only widespread but also achieved noticeable results on numerous applications including image classification, restoration, and generation. Although the weight-sharing property of convolutions makes them widely adopted in various tasks, its content-agnostic characteristic can also be considered a major drawback. To solve this problem, in this paper, we propose a novel operation, called pixel adaptive kernel attention (PAKA). PAKA provides directivity to the filter weights by multiplying spatially varying attention from learnable features. The proposed method infers pixel-adaptive attention maps along the channel and spatial directions separately to address the decomposed model with fewer parameters. Our method is trainable in an end-to-end manner and applicable to any CNN-based models. In addition, we propose an improved information aggregation module with PAKA, called the hierarchical PAKA module (HPM). We demonstrate the superiority of our HPM by presenting state-of-the-art performance on semantic segmentation compared to the conventional information aggregation modules. We validate the proposed method through additional ablation studies and visualizing the effect of PAKA providing directivity to the weights of convolutions. We also show the generalizability of the proposed method by applying it to multi-modal tasks especially color-guided depth map superresolution.

Index Terms—Deep learning, Content-adaptive convolution, Semantic segmentation, Color-guided depth map super-resolution

I. INTRODUCTION

EEP learning based on convolutional neural networks (CNNs) has brought remarkable improvement to image processing and computer vision tasks including object detection [1]–[6], classification [7]–[11], image restoration [12]–[16], and generation [17]–[21]. Convolution is a basic element of CNNs, and has been considered as one of the most effective methods to extract and propagate features from images. Due to its weight sharing property, CNNs require less parameters than fully-connected layer and can be efficiently optimized by GPU implementation. However, the learned filters stay fixed after training in traditional convolution, making operation contentagnostic.

Toward content-adaptive convolution, a learnable filter which is generated dynamically conditioned on input features was proposed and showed promising effectiveness through the quantitative and qualitative performance evaluation [2], [22], [23]. In particular, with the marginal increase in the

Corresponding author: Seung-Won Jung.

M.-C. Sagong, Y.-J. Yeo, S.-W. Jung, and S.-J. Ko are with School of Electrical Engineering Department, Korea University, Anam-dong, Sungbukgu, Seoul, 136-713, Rep. of Korea (e-mail: mcsagong@dali.korea.ac.kr, yjyeo@dali.korea.ac.kr, swjung83@korea.ac.kr, sjko@korea.ac.kr).

number of network parameters, its adaptive property improves flexibility of the model. Moreover, Su et al. [23] introduced a pixel-adaptive convolution (PAC) which multiplies a spatiallyvarying kernel with the shared filter weights. It can be ideally used for a wide range of tasks but its effectiveness was shown for only a few image filtering tasks. To further improve flexibility of convolution, a deformable convolution [2], in which spatial sampling locations are augmented with additional learnable offsets, was proposed. This helps CNNs enhance the transformation modeling capability without additional supervision. To focus more precisely on pertinent image regions, the deformable convolution was further reformulated by modulating the input feature amplitudes according to the spatial locations and bins [24]. This modulation can prevent features to be influenced by irrelevant content outside the region of interest.

In this paper, we propose a novel convolutional operation, called pixel adaptive kernel attention (PAKA), which drives the standard convolution to handle a content-adaptive receptive field. Specifically, PAKA modifies the weights of convolution with directional and channel modulations. The directional modulation emphasizes or suppresses features from different kernel directions while channel modulation aggregates the inter-channel relationship. With PAKA, the convolution predicts directions that provide pertinent information in every pixel. We evaluate the efficacy of PAKA with various experiments on multiple tasks. For the semantic segmentation task, we propose a hierarchical module with PAKA which can utilize diverse effective patch sizes. Through the proposed module, the network learns to attend to content-adaptive directions to inherit more information. To visually demonstrate this behavior, we define the modulated receptive field, called propagational field, which is emphasized or suppressed receptive field by the directional modulation. We validate our module by comparing ours with the state-of-the-art information aggregation modules under the same conditions. To demonstrate the generalizability of our method, we also apply PAKA to the joint up-sampling layer for the color-guided depth map super-resolution task. The experimental results indicate that the proposed method not only exhibits superiority on various CNN-based tasks but also has a noticeable potential.

In summary, in this paper we present:

- A novel convolutional operation that provides directivity to the standard convolution to address its limitation which is content-agnostic.
- A novel information aggregation module and extensive experiments to validate the effectiveness of the proposed method on semantic segmentation.

 Application of the proposed method to the joint upsampling layer and extensive experiments to validate its effectiveness on color-guided depth map super-resolution.

II. RELATED WORKS

Content-adaptive filters Recently, several works have explored the idea of utilizing effective content-adaptive filtering techniques such as bilateral filtering [25], [26] and guided filtering [27] as the layers of the CNNs. In the early stages in this direction, some approaches [28], [29] made these filters differentiable to back-propagate the gradients for learning network parameters. Moreover, the learnable layers that play the role of the bilateral filter were applied to superpixels [30]. On the other hand, by reformulating the guided filter as a fully differentiable block, Wu et al. [31] proposed guided filtering layers that can be jointly optimized through end-toend training. While the aforementioned methods cannot fully replace the standard convolution by their proposed layers, Jampani et al. [32] introduced a sparse high-dimensional convolution that modifies the standard convolution to be contentadaptive. Similarly, Su et al. [23] presented a generalized convolution, called PAC, which can learn adaptive filters and has less computational overhead compared to [32]. In addition, introduced by Jia et al. [22], the dynamic filter network (DFN) directly predicts filter weights using a separate network branch; thus, it can generate adaptive filters corresponding to each input feature.

Attention mechanisms In learning a series of pattern recognition tasks, depending on the characteristic of each task, the network should reflect that given feature maps have different importance along spatial and/or channel direction. To this end, there have been several attempts to adopt the attention modules, which compute the responses for the local part while attending to the global context. Wang et al. [33] introduced a residual attention module which directly generates 3D attention map to refine the intermediate feature map. By using this module, the network performs robustly against noisy labels. Meanwhile, Hu et al. [34] proposed a squeezeand-excitation module that computes channel attention with global average pooling. Even though the architecture effectively exploits the inter-channel relationships, they did not consider the spatial attention which plays an important role in inferring accurate attention for 3D feature maps. On the other hand, some approaches [35], [36] separately learn both channel attention and spatial attention. By applying the decomposed attention generation, the network showed superior performance than [34] as well as much less parameter overhead than [33].

Information aggregation modules In recent years, many researches have explored information aggregation for scene understanding. Zhao *et al.* [37] proposed PSPNet which adopts the pyramid spatial pooling (PSP) module [38] to reduce the feature maps into different scales. PSPNet utilizes various local context including the global information. On the other hand, Deeplab methods [39]–[41] introduced atrous spatial pyramid pooling (ASPP) which applies sampling with different rates for information aggregation. Fu *et al.* [42] and Yuan *et al.* [43] adopted the self-attention mechanism [44] to aggregate

long-range spatial information, while Zhang *et al.* [45] utilized context encoding module (CEM) which contains the global pooling to capture the global context and highlights the class-dependent feature maps.

III. PROPOSED METHOD

Fig. 1 illustrates the modified convolution in which PAKA is applied. The proposed method produces kernel attention from input feature through two separate branches, *i.e.*, channel modulation branch and directional modulation branch. In this section, we describe details of PAKA.

A. Pixel Adaptive Kernel Attention

Formally, convolution for each location p on the output feature map $y \in \mathbb{R}^{H \times W}$ and input feature maps $x \in \mathbb{R}^{N \times H \times W}$ can be expressed as follows:

$$y(p) = \sum_{j=1}^{N} \sum_{k=1}^{K} x(p + p_k, j) \cdot w(k, j), \tag{1}$$

where w(k,j) denotes the weight for the k-th location and the j-th channel, and p_k is the pre-specified offset for the k-th location. N and K are the numbers of channels and sampling locations, respectively. For instance, K=9 and $p_k \in \{(-1,-1),(-1,0),\ldots,(1,1)\}$ correspond to 3×3 convolution with dilation 1. (1) indicates that the weights only depend on pixel and channel positions; thus, the standard convolution is content-agnostic. To cope with this problem, we designed PAKA which provides directivity to weights along pixel contents. With PAKA, (1) becomes

$$y(p) = \sum_{i=1}^{N} \sum_{k=1}^{K} x(p + p_k, j) \cdot w(k, j) \cdot A_{k,j}(p),$$
 (2)

where $A_{k,j}$ is learnable kernel attention for the k-th location and the j-th channel. The attention lies in the bounded range by applying the activation function to the combination of directional and channel modulations, which are denoted as $m_k \in \mathbb{R}^{K \times H \times W}$ and $n_j \in \mathbb{R}^{N \times H \times W}$, respectively. Each modulation is obtained by individual branches that apply multiple learnable layers to the same input feature maps x. By combining two decomposed modulations, PAKA can conduct attention mechanism in an efficient and effective manner. In particular, we apply element-wise summation with the tensor broadcast to combine them for efficient gradient flow [8]. As a result, the kernel attention can be expressed as

$$A_{k,i} = 1 + \tanh(m_k + n_i).$$
 (3)

Channel modulation branch Each pixel in feature maps contains information from different contents (e.g., pixels from the object and background). As each channel tends to respond to a specific feature, we drive PAKA to exploit inter-channel relationship from every single pixel by channel modulation. We use a multi-layer perceptron including two 1×1 convolutional layers followed by a batch normalization layer to estimate channel modulation.

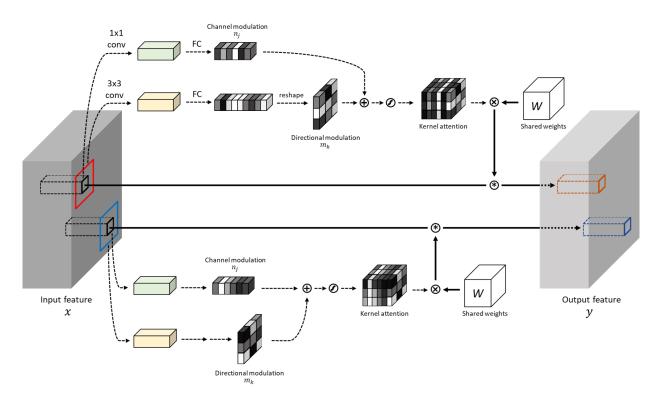


Fig. 1. Details of PAKA. Given the intermediate feature map x, PAKA computes the channel modulation n_j and directional modulation m_k through the two separate branches in every pixel. Both branches contain a couple of convolutional layers, the batch normalization, and ReLU. The two modulations are combined with the tensor broadcast and generate the kernel attention by the activation function. Since the kernel attention is different in every pixel, the proposed convolutional layer can learn the content-adaptive directivity.

Directional modulation branch Pixels corresponding to the same object can be surrounded by different objects (e.g., pixels in the center and around boundary of objects). However, since the standard convolution applies shared weights across every pixel, a trained network propagates information from the same directions for different pixels in an image. To solve this problem, the directional modulation m_k is acquired to emphasize or suppress information from different directions. Specifically, it infers which kernel direction among the prespecified offsets should be focused on every pixel. By adopting multiple convolutional layers with PAKA, each pixel can take information propagated from different fields. We design the directional modulation branch using a 3×3 convolutional layer followed by a 1×1 convolutional layer. In particular, the $3 \times$ 3 layer is designed to have the same kernel size, dilation, and stride as the shared convolution layer such that they have the same receptive field. In addition, batch normalization is applied at the end of convolutional layer for a scale adjustment.

B. Hierarchical PAKA Module

With PAKA, we propose our hierarchical PAKA module, or HPM, as illustrated in Fig. 2. On the top of the module, we apply a 1×1 convolutional layer with BN and ReLU to squeeze the number of channels before feeding into the convolutional layers with PAKA. The HPM employs a series of dilated convolutional layers with PAKA to deal with the hierarchical pyramid architecture in fixed size feature maps. Using dilated convolutional layers with increasing dilation rates, the module covers diverse receptive fields as similar to the hierarchical

pyramid architecture. In the last of HPM, we concatenate the Globally pooling input and every output feature maps from PAKA with different dilation rates.

C. Understanding and Analysis

Several existing convolution operations perform position-specific modifications as explained in Section II. In DFN [22], since an auxiliary network generates filters for every offset and channel, a large number of parameters are needed. In addition, DFN requires an elaborate architecture design because all position-specific filter weights have to be predicted without sharing. Unlike DFN, PAKA allows efficient learning by position-specific attentions and shared weights. Liu *et al.* [46] and Cheng *et al.* [47] propose spatial propagation networks by learning affinity. Although they utilize the directivity to propagate the information, they target the guide learning or refinement to learn affinity matrices. On the contrary, PAKA can be self-directed because it only specifies the direction to focus on each pixel.

The deformable convolution [2], [24] employs position-specific modification by altering the grid of convolutional kernel to apply different sizes of receptive fields on different targets. It augments the spatial sampling location with the learnable offsets and modulation scalars. However, since the offset vectors have a high degree of freedom, it is very challenging to reach an optimal solution. In addition, the deformable convolution cannot explicitly consider the channel-wise attention because it only modifies the spatial sampling

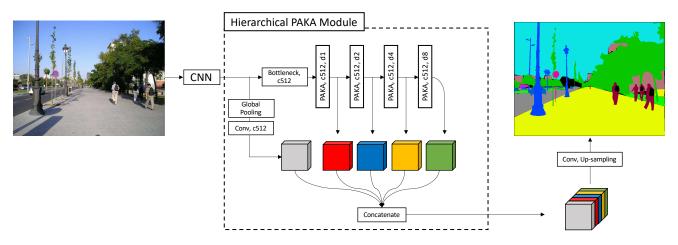


Fig. 2. An architecture of HPM. We apply the bottleneck layer to reduce the channel of input feature maps before feeding into the first PAKA layer. The module contains several PAKA layers with different dilation rates. We indicate PAKA layers' output channel with c and dilation rate with d. We concatenate the input and output features of each PAKA layer to utilize various receptive fields.

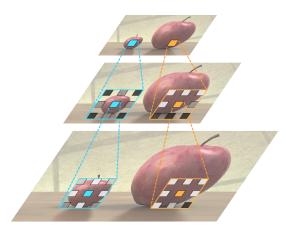


Fig. 3. Toy example for multiple convolutional layers with PAKA on different locations. With PAKA, the convolution propagates the information from different directions depending on the local contents.

location. Fig. 3 shows how PAKA applies different effective receptive fields with kernel attention. We adopt PAKA in a hierarchical pyramid architecture to adjust effective receptive fields by regulating kernel attention in different layers. Consequently, various effective patch sizes can be utilized even with adoption of the fixed kernel size. As a result, PAKA drives the network to take information from different effective receptive fields depending on the contents.

Figs. 4 and 5 visualize the modulated receptive fields obtained by PAKA, named propagational field. Here, the propagational field is visualized by adding 8-neighborhood sampling offsets multiplied by the directional modulation from every PAKA layer to indicate which directions received high attention. Fig. 4 illustrates the propagational fields of two pixels on different objects. As can be seen especially from Fig. 4(b), the propagational fields of the adjacent pixels on the human and the background are clearly distinguished. In addition, Fig. 5 demonstrates that even pixels corresponding to the same contents inherit information from different propagational fields depending on their locations.

IV. EXPERIMENTAL RESULTS

The proposed method is evaluated on the ADE20K [48] dataset for the semantic segmentation task. The ADE20K dataset contains very challenging 150 classes including 35 stuff classes and 115 discrete object classes. The dataset is divided into 20,210 images for training, 2,000 and 3,352 images for validation and testing, respectively. For evaluation, class-wise intersection over union (mIoU) and pixel-wise accuracy (PixAcc) are used.

A. Implementation Details

As a backbone network for feature extraction, we use a pretrained ResNet [8] model with the dilated network strategy [39], [49]. The size of the feature maps is 1/8 of the size of the input image. We adopt convolutional layers and bilinear up-sampling layer to generate the final prediction map. We apply the cross-entropy loss to train the proposed network. Following the previous researches [37], we integrate the auxiliary loss in stage 4 of the ResNet backbone.

For the training, we normalize the input in the range [-1,1]. We also apply data augmentation including random horizontal flipping, random Gaussian filtering, and scaling with random factors of [0.5,2.0] to avoid overfitting. Last, we randomly crop the input image into the fixed size of 256×256 pixels. The pioneering researches [37], [45] mention that the larger the crop size, the better the semantic segmentation performance. However, we use the same patch size of 256×256 for all compared methods considering our hardware resource. Although it is smaller than the size used in the original papers, whole conditions are unified for fair validation of the information aggregation modules.

During the training phase, we employ the stochastic gradient descent algorithm with a poly learning rate policy, $\gamma = \gamma_0 \times (1 - \frac{N_{iter}}{N_{total}})^p$, where N_{iter} and N_{total} represent the current iteration number and total iteration number, respectively, and p=0.9. We set the initial learning rate γ_0 as 0.01, momentum as 0.9, weight decay as 0.0001, and batch size as 16. We train the model for 150K iterations.





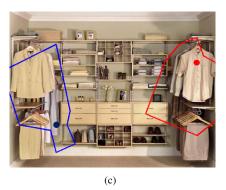




Fig. 4. Visualization of the propagational fields corresponding to the marked pixels. Each sub-figure shows the propagational fields of the pixels on different contents.

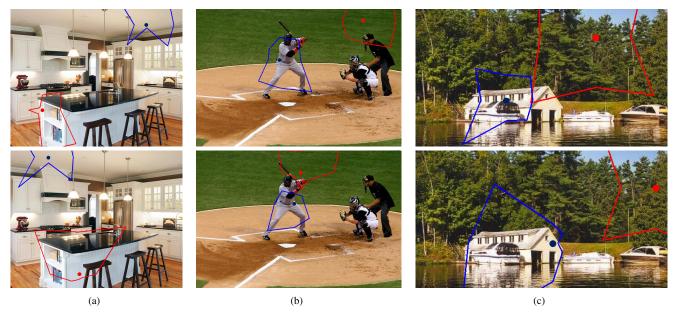


Fig. 5. Visualization of the propagational fields corresponding to the marked pixels. Each sub-figure shows the changes of the propagational fields when pixel location is changed even in the same object.

B. Evaluation for Semantic Segmentation

Ablation Study for HPM To demonstrate the superiority of our PAKA and HPM, we conduct the experiments with several different settings containing the conventional information aggregation modules, which are PSP [37], ASPP [40] and, Self-Attention [44], as shown in Table I.

First, we evaluate performance of our baseline model. The baseline consists of ResNet for the backbone network and the last convolutional layers followed by a up-sampling layer. It results in 36.28% in terms of mIoU and 76.84% in terms of PixAcc. We adopt this model as our baseline to compare the performance of the information aggregation modules. We list our evaluation results of different information aggregation modules in Table I. Note that we reimplement the conventional methods using the same condition for fair comparison. As can be seen in the table, the proposed method shows the best result in terms of both mIoU and PixAcc. With our HPM, the baseline model is significantly improved by 4.87% and 2.86% in terms of mIoU and PixAcc, respectively. Fig. 6 shows several semantic segmentation results obtained by the baseline

and HPM, demonstrating the effectiveness of information aggregation by HPM.

In order to demonstrate the validity of the proposed modulations, we conducted ablation experiments by eliminating each modulation from PAKA. Table II shows that the PAKA without any modulation exhibits inferior performance compared with the original PAKA and both modulations are essential for the performance improvement. To support the effectiveness of PAKA and the necessity of HPM, we have conducted ablation studies by switching the standard convolution and PAKA in ASPP and HPM. As shown in Table III, simple replacement of the standard convolution by PAKA improves the performance of ASPP. In addition, it shows that PAKA is more effective with HPM compared to ASPP. We consider this is because a cascade structure with PAKA can utilize diverse propagational fields as illustrated in Fig. 3. However, ASPP adopts a parallel structure that cannot fully take advantage of PAKA. Therefore, we designed HPM including a cascade structure with PAKA to fully exploit its effectiveness. Moreover, to show the computational cost of PAKA, we present the number of parameters and

TABLE I
SEGMENTATION RESULTS ON THE ADE20K VALIDATION SET IN
COMPARISON WITH DIFFERENT INFORMATION AGGREGATION MODULES.

model	mIOU	pixAcc
ResNet-50 (Baseline)	36.28	76.84
ResNet-50 + PSP	38.34	77.79
ResNet-50 + Self-Attention	39.16	78.58
ResNet- $50 + ASPP$	40.37	79.39
ResNet-50 + HPM (Proposed)	41.15	79.70
ResNet-101 (Baseline)	39.03	78.60
ResNet-101 + PSP	40.12	79.55
ResNet-101 + Self-Attention	41.84	80.08
ResNet-101 + ASPP	42.08	80.07
ResNet-101 + HPM (Proposed)	42.21	80.38

TABLE II
ABLATION STUDY DEMONSTRATING THE EFFECTS OF CHANNEL
MODULATION AND DIRECTIONAL MODULATION.

Channel	Directional	mIOU	pixAcc
		39.85	78.43
\checkmark		40.41	79.68
	✓	40.85	79.65
\checkmark	✓	41.15	79.70

TABLE III
ABLATION STUDY REPLACING STANDARD CONVOLUTION
WITH PAKA FOR ASPP AND REPLACING PAKA WITH STANDARD
CONVOLUTION FOR HPM.

Backbone	ResNet-50			
Aggregation module	ASPP		HPM	
PAKA		✓		✓
# parameters	56.0M	90.7M	36.1M	40.8M
average runtime	138ms	187ms	124ms	136ms
mIOU	40.37	<u>40.71</u>	39.85	41.15

the runtime of ASPP and HPM in Table III. ASPP requires much more parameters than HPM for the adoption of PAKA. This is because ASPP adopts a parallel structure with 2,048 input channels for every layer but HPM adopts a cascade structure with 512 input channels. As a result, we verify that PAKA improves not only the conventional aggregation module such as ASPP but also HPM more significantly with much less parameter increment.

We also evaluate the combined model of HPM and the conventional modules. As mentioned in Section III-C, HPM learns direction to propagate the context information. Since HPM plays a different role compared to other modules, combining HPM with the other existing modules can yield further improvement. As indicated in Table IV, the combined module produces better results than a single module.

Comparison with state-of-the-art methods We compare the proposed method with other state-of-the-art methods to demonstrate effectiveness of the proposed method. For this experiment, we use the same patch size as the conventional methods (480×480) for training and utilize the combined model of ASPP and HPM. Similar to the compared methods [37], [40], [50], [51], we average the predictions from multiple scaled and flipped inputs to further improve the performance. We use the scale factors of $\{0.5, 0.75, 1.0, 1.25, 1.5\}$ for the

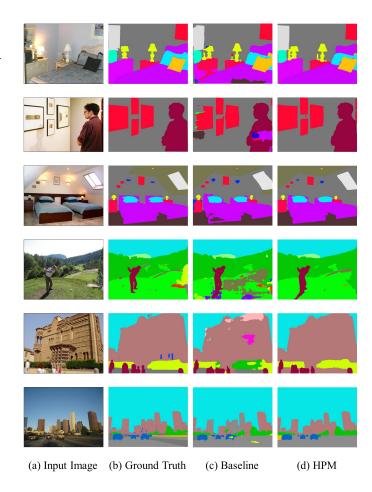


Fig. 6. Qualitative comparisons with the baseline and HPM on the ADE20K validation dataset. Propagation of the related context information by PAKA helps to understand the scenes, resulting in a significantly performance improvement over the baseline.

TABLE IV PERFORMANCE IMPROVEMENTS BY COMBINING HPM WITH THE CONVENTIONAL MODULES. THE EVALUATION METRIC IS MIOU(%). Δ INDICATES THE ABSOLUTE DIFFERENCE.

	PSP	Self-Attention	ASPP
w/o HPM	38.34	39.16	40.37
w/ HPM	41.48	41.02	41.47
Δ	↑3.14	↑1.86	↑1.10

multi-scale testing strategy. As shown in Table V, the proposed method outperforms recent state-of-the-art methods although our proposed method is trained with simple up-sampling layers for image reconstruction.

V. JOINT DEPTH SUPER-RESOLUTION WITH PAKA

In order to demonstrate superiority over other content-adaptive convolution, *i.e.*, pixel-adaptive convolution (PAC), and generalizability of PAKA, as a case study, we apply PAKA for the color-guided depth map super-resolution task, which generates a high-resolution depth map with help of its corresponding high-resolution color image. Early studies adopt content-adaptive filtering techniques such as joint bilateral filtering [56] and guided image filtering [27]. The common

TABLE V QUANTITATIVE EVALUATION ON THE ADE20K VALIDATION SET IN COMPARISON WITH STATE-OF-THE-ART METHODS.

Method	Backbone	mIOU	pixAcc
EncNet [45]	ResNet-50	41.11	79.73
PSPNet [37]	ResNet-50	42.78	80.76
ACNet [50]	ResNet-50	43.01	81.01
CFNet [52]	ResNet-50	42.87	-
CPN [51]	ResNet-50	44.46	81.38
Proposed	ResNet-50	44.75	81.61
PSPNet [37]	ResNet-101	43.29	81.39
PSANet [53]	ResNet-101	43.77	81.51
EncNet [45]	ResNet-101	44.65	81.19
CFNet [52]	ResNet-101	44.89	-
ANL [54]	ResNet-101	45.24	-
OCR [43]	ResNet-101	45.28	-
APCNet [55]	ResNet-101	45.38	-
Proposed	ResNet-101	45.42	81.88

characteristic of them is that they determine filter weights to up-sample the target (*i.e.*, low-resolution (LR) depth map) from the guide content (*i.e.*, HR color image). Consequently, the surrounding pixels that have higher content similarity to the center have greater influence in filtering. We notice that PAKA can be used as a learnable and generalized model of such conventional filtering methods.

A. Joint up-sampling layer with PAKA

To conduct the color-guided depth map super-resolution task, we design a joint up-sampling layer with PAKA. Fig. 7 illustrates the proposed joint up-sampling layer with PAKA. The proposed joint up-sampling layer receives low-resolution (LR) target feature maps and high-resolution (HR) guide feature maps as input. We obtain the kernel attentions from the guide feature maps by employing both channel modulation branch and directional modulation branch in the same manner as the original PAKA. The each kernel attention is multiplied with the shared weights to generate sub-pixels of the upsampled feature maps. With the kernel attention from PAKA, the proposed joint up-sampling layer is driven to concentrate more on important directions (e.g. edge) to inherit the information from the guide features.

B. Implementation Details

We build the network architecture motivated by the pioneering method [57] of joint depth map super-resolution, which is simple yet efficient. We provide the details of the network in Fig. 8. Following the common training procedure [57], [58], we use MPI Sintel depth dataset [59] and Middlebury dataset [60] (including 2001, 2006 and 2014 datasets). In the training phase, we crop the images into 128×128 patches with overlapping for all scaling factors (*i.e.* $\times 8$ and $\times 16$) to reduce the training time.

C. Evaluation for depth map super-resolution

Table VI shows the numeric results of the proposed and conventional methods in case of 8 times and 16 times super-resolution, respectively. We compare the performance in terms of *root mean squared error* (RMSE) and *peak signal-to-noise*

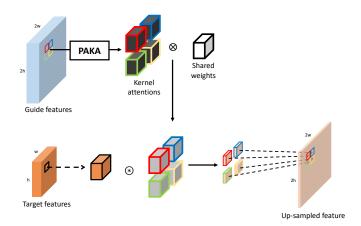


Fig. 7. Framework of the proposed joint up-sampling layer with PAKA for depth map super-resolution. The proposed joint up-sampling layer generate 4 sub-pixels from LR target feature maps for $\times 2$ up-sampling.

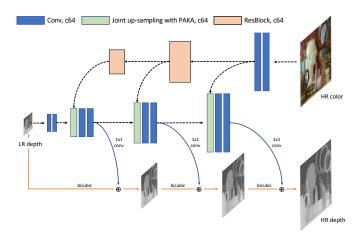


Fig. 8. Architecture of the proposed color guided depth-map super-resolution network for $\times 8$ up-sampling. We apply our joint up-sampling layer in Fig. 7 to the architecture motivated from the MSG-Net [57].

ratio (PSNR). As can be seen in the table, our proposed joint up-sampling network with PAKA outperforms the conventional state-of-the-art methods [23], [58], [61]. For further study, we test the conventional methods in conjunction with PAKA. As can be seen in Table VII, PAKA contributes to further performance improvements of the conventional models. Fig. 9 shows visual comparisons of the state-of-the-art methods and the proposed method. The proposed method generates more sharp object boundaries than other methods. It indicates that PAKA can help to learn accurate directivity to up-sample the features than the conventional methods.

VI. CONCLUSION

In this paper, we propose a novel convolutional operation called PAKA that learns the directivity to effectively propagate information. PAKA emphasizes or suppresses information from different directions with two decomposed branches, which predict channel and directional modulations. We validate superiority of PAKA with visualization of its propagational fields and the extensive experiments. We also demonstrate that PAKA is applicable in many vision tasks

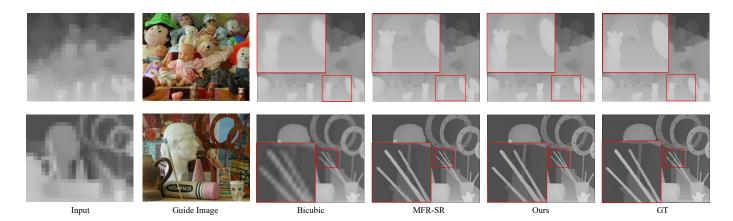


Fig. 9. Visual comparison results at $\times 16$ up-sampling for "Dolls" and "Art" in the Middlebury dataset. The regions inside the red boxes are magnified for comparison.

TABLE VI QUANTITATIVE COMPARISON ON THE MIDDLEBURY DATASET FOR $\times 8$ (TOP) AND $\times 16$ (BOTTOM) SCALING FACTORS IN TERMS OF RMSE/PSNR (DB).

Method	Art	Books	Dolls	Laundry	Moebius	Reindeer	Average
Bicubic	5.47 / 33.37	2.34 / 40.75	1.87 / 42.69	3.42 / 37.45	1.96 / 42.29	4.01 / 36.07	3.18 / 38.01
TGV [62]	7.02 / 31.20	2.08 / 41.77	2.05 / 41.90	3.92 / 36.27	2.41 / 40.49	4.29 / 35.48	3.63 / 37.85
SRCNN [13]	4.75 / 34.60	2.15 / 41.48	1.92 / 42.46	3.45 / 37.37	2.00 / 42.11	3.87 / 36/38	3.02 / 38.52
MSG-Net [57]	2.63 / 39.73	1.16 / 46.87	1.67 / 43.79	1.67 / 43.69	1.21 / 46.51	1.97 / 42.24	1.64 / 43.81
Depth-SR [58]	2.39 / 40.58	1.04 / 47.75	1.22 / 46.37	1.43 / 45.03	1.10 / 47.27	1.78 / 43.14	1.43 / 45.02
MFR-SR [61]	2.29 / 40.94	1.02 / 47.98	1.22 / 46.38	1.41 / 45.15	1.10 / 47.27	1.68 / 43.61	1.40 / 45.22
PAC [23]	2.36 / 40.67	1.05 / 47.74	1.24 / 46.23	1.40 / 45.22	1.10 / 47.32	1.66 / 43.73	1.41 / 45.15
Proposed	2.26 / 41.04	0.83 / 49.71	1.12 / 47.16	1.30 / 45.83	0.89 / 49.15	1.61 / 44.01	1.26 / 46.15
Method	Art	Books	Dolls	Laundry	Moebius	Reindeer	Average
Diaukia	9 17 / 20 90	2 24 / 27 65	2 64 / 20 70	5 07 / 24 04	2.95 / 20.02	5 96 1 22 77	16612177

Method	Art	Books	Dolls	Laundry	Moebius	Reindeer	Average
Bicubic	8.17 / 29.89	3.34 / 37.65	2.64 / 39.70	5.07 / 34.04	2.85 / 39.03	5.86 / 32.77	4.66 / 34.77
TGV [62]	12.08 / 26.49	4.89 / 34.34	4.44 / 35.18	8.01 / 30.06	5.41 / 33.47	9.05 / 29.00	7.31 / 31.42
SRCNN [13]	7.80 / 30.29	3.24 / 37.91	2.61 / 39.80	5.04 / 34.08	2.82 / 39.13	5.63 / 33.12	4.52 / 35.02
MSG-Net [57]	4.25 / 35.57	1.85 / 42.81	1.77 / 43.19	2.92 / 38.81	1.79 / 43.05	3.18 / 38.09	2.48 / 40.25
Depth-SR [58]	4.09 / 35.89	1.65 / 43.78	1.68 / 43.63	2.31 / 40.86	1.66 / 43.71	2.68 / 39.58	2.21 / 41.24
MFR-SR [61]	3.55 / 37.13	1.60 / 44.06	1.62 / 43.95	2.18 / 41.35	1.58 / 44.18	2.35 / 40.70	2.05 / 41.90
PAC [23]	3.75 / 36.66	1.64 / 43.86	1.62 / 43.92	2.28 / 40.96	1.53 / 44.42	2.59 / 39.87	2.12 / 41.62
Proposed	3.58 / 37.04	1.44 / 44.98	1.54 / 44.36	2.17 / 41.39	1.44 / 44.97	2.43 / 40.41	1.98 / 42.19

TABLE VII DIRECT REPLACEMENT RESULTS WITH THE CONVENTIONAL METHODS ON THE DEPTH MAP SUPER RESOLUTION IN TERMS OF AVERAGE PSNR (DB).

Method	PSNR (×8)	PSNR (×16)
MSG-Net [57]	43.81	40.25
MSG-Net w/ PAKA	44.58	41.66
PAC-Net [23]	45.15	41.61
PAC-Net w/ PAKA	45.31	41.75
Proposed	45.78	41.91

including semantic segmentation and joint depth map superresolution. Since PAKA can directly replace the standard convolutional layers, we think that PAKA has a notable potential to leverage various CNN-based tasks.

REFERENCES

- [1] R. Girshick, "Fast R-CNN," in *Proceedings of the IEEE International Conference on Computer Vision*, 2015, pp. 1440–1448. 1
- [2] J. Dai, H. Qi, Y. Xiong, Y. Li, G. Zhang, H. Hu, and Y. Wei, "Deformable convolutional networks," in *Proceedings of the IEEE International Conference on Computer Vision*, 2017, pp. 764–773. 1, 3

- [3] H. Law and J. Deng, "Cornernet: Detecting objects as paired keypoints," in *Proceedings of the European Conference on Computer Vision*, 2018, pp. 734–750.
- [4] Y. Cao, K. Chen, C. C. Loy, and D. Lin, "Prime sample attention in object detection," in *Proceedings of the IEEE Conference on Computer Vision and Pattern Recognition*, June 2020.
- [5] M. Tan, R. Pang, and Q. V. Le, "EfficientDet: Scalable and efficient object detection," in *Proceedings of the IEEE Conference on Computer Vision and Pattern Recognition*, June 2020.
- [6] Y. Ji, H. Zhang, Z. Jie, L. Ma, and Q. J. Wu, "Casnet: A cross-attention siamese network for video salient object detection," *IEEE transactions* on neural networks and learning systems, vol. 32, no. 6, pp. 2676–2690, 2020.
- [7] K. Simonyan and A. Zisserman, "Very deep convolutional networks for large-scale image recognition," arXiv preprint arXiv:1409.1556, 2014.
- [8] K. He, X. Zhang, S. Ren, and J. Sun, "Deep residual learning for image recognition," in *Proceedings of the IEEE Conference on Computer Vision* and Pattern Recognition, 2016, pp. 770–778. 1, 2, 4
- [9] C. Szegedy, W. Liu, Y. Jia, P. Sermanet, S. Reed, D. Anguelov, D. Erhan, V. Vanhoucke, and A. Rabinovich, "Going deeper with convolutions," in *Proceedings of the IEEE Conference on Computer Vision and Pattern Recognition*, 2015, pp. 1–9.
- [10] Q. Xie, M.-T. Luong, E. Hovy, and Q. V. Le, "Self-training with noisy student improves imagenet classification," in *Proceedings of the IEEE* Conference on Computer Vision and Pattern Recognition, 2020, pp. 10 687–10 698.

- [11] C. Zhang, Y. Cai, G. Lin, and C. Shen, "DeepEMD: Few-shot image classification with differentiable earth mover's distance and structured classifiers," in *Proceedings of the IEEE Conference on Computer Vision* and Pattern Recognition, June 2020.
- [12] M.-c. Sagong, Y.-g. Shin, S.-w. Kim, S. Park, and S.-j. Ko, "PEPSI: Fast image inpainting with parallel decoding network," in *Proceedings of the IEEE Conference on Computer Vision and Pattern Recognition*, 2019, pp. 11360–11368.
- [13] C. Dong, C. C. Loy, K. He, and X. Tang, "Image super-resolution using deep convolutional networks," *IEEE Transactions on Pattern Analysis* and Machine Intelligence, vol. 38, no. 2, pp. 295–307, 2015. 1, 8
- [14] Y.-J. Yeo, Y.-G. Shin, M.-C. Sagong, S.-W. Kim, and S.-J. Ko, "Simple yet effective way for improving the performance of lossy image compression," *IEEE Signal Processing Letters*, vol. 27, pp. 530–534, 2020.
- [15] S. W. Zamir, A. Arora, S. Khan, M. Hayat, F. S. Khan, M.-H. Yang, and L. Shao, "CycleISP: Real image restoration via improved data synthesis," in *Proceedings of the IEEE Conference on Computer Vision and Pattern Recognition*, June 2020. 1
- [16] M. Suin, K. Purohit, and A. N. Rajagopalan, "Spatially-attentive patchhierarchical network for adaptive motion deblurring," in *Proceedings of* the IEEE Conference on Computer Vision and Pattern Recognition, June 2020. 1
- [17] I. Goodfellow, J. Pouget-Abadie, M. Mirza, B. Xu, D. Warde-Farley, S. Ozair, A. Courville, and Y. Bengio, "Generative adversarial nets," in Proceedings of the Advances in Neural Information Processing Systems, 2014, pp. 2672–2680.
- [18] L. A. Gatys, A. S. Ecker, and M. Bethge, "Image style transfer using convolutional neural networks," in *Proceedings of the IEEE Conference* on Computer Vision and Pattern Recognition, 2016, pp. 2414–2423. 1
- [19] P. Zhu, R. Abdal, Y. Qin, and P. Wonka, "SEAN: Image synthesis with semantic region-adaptive normalization," in *Proceedings of the IEEE Conference on Computer Vision and Pattern Recognition*, June 2020.
- [20] C.-H. Lee, Z. Liu, L. Wu, and P. Luo, "MaskGAN: Towards diverse and interactive facial image manipulation," in *Proceedings of the IEEE* Conference on Computer Vision and Pattern Recognition, June 2020. 1
- [21] Y.-G. Shin, M.-C. Sagong, Y.-J. Yeo, S.-W. Kim, and S.-J. Ko, "Pepsi++: Fast and lightweight network for image inpainting," *IEEE Transactions on Neural Networks and Learning Systems*, vol. 32, no. 1, pp. 252–265, 2020.
- [22] X. Jia, B. De Brabandere, T. Tuytelaars, and L. V. Gool, "Dynamic filter networks," in *Proceedings of the Advances in Neural Information Processing Systems*, 2016, pp. 667–675. 1, 2, 3
- [23] H. Su, V. Jampani, D. Sun, O. Gallo, E. Learned-Miller, and J. Kautz, "Pixel-adaptive convolutional neural networks," in *Proceedings of the IEEE Conference on Computer Vision and Pattern Recognition*, 2019, pp. 11166–11175. 1, 2, 7, 8
- [24] X. Zhu, H. Hu, S. Lin, and J. Dai, "Deformable convnets v2: More deformable, better results," in *Proceedings of the IEEE Conference on Computer Vision and Pattern Recognition*, 2019, pp. 9308–9316. 1, 3
- [25] C. Tomasi and R. Manduchi, "Bilateral filtering for gray and color images," in *Proceedings of the IEEE International Conference on Computer Vision*, 1998, pp. 839–846.
- [26] V. Aurich and J. Weule, "Non-linear Gaussian filters performing edge preserving diffusion," in *Mustererkennung 1995*. Springer, 1995, pp. 538–545.
- [27] K. He, J. Sun, and X. Tang, "Guided image filtering," *IEEE Transactions on Pattern Analysis and Machine Intelligence*, vol. 35, no. 6, pp. 1397–1409, 2012. 2, 6
- [28] L.-C. Chen, A. Schwing, A. Yuille, and R. Urtasun, "Learning deep structured models," in *Proceedings of the International Conference on Machine Learning*, 2015, pp. 1785–1794.
- [29] S. Zheng, S. Jayasumana, B. Romera-Paredes, V. Vineet, Z. Su, D. Du, C. Huang, and P. H. Torr, "Conditional random fields as recurrent neural networks," in *Proceedings of the IEEE International Conference on Computer Vision*, 2015, pp. 1529–1537.
- [30] R. Gadde, V. Jampani, M. Kiefel, D. Kappler, and P. V. Gehler, "Super-pixel convolutional networks using bilateral inceptions," in *Proceedings of the European Conference on Computer Vision*, 2016, pp. 597–613.
- [31] H. Wu, S. Zheng, J. Zhang, and K. Huang, "Fast end-to-end trainable guided filter," in *Proceedings of the IEEE Conference on Computer* Vision and Pattern Recognition, 2018, pp. 1838–1847.
- [32] V. Jampani, M. Kiefel, and P. V. Gehler, "Learning sparse high dimensional filters: Image filtering, dense CRFs and bilateral neural networks," in *Proceedings of the IEEE Conference on Computer Vision and Pattern Recognition*, 2016, pp. 4452–4461.

- [33] F. Wang, M. Jiang, C. Qian, S. Yang, C. Li, H. Zhang, X. Wang, and X. Tang, "Residual attention network for image classification," in *Proceedings of the IEEE Conference on Computer Vision and Pattern Recognition*, 2017, pp. 3156–3164.
- [34] J. Hu, L. Shen, and G. Sun, "Squeeze-and-excitation networks," in Proceedings of the IEEE Conference on Computer Vision and Pattern Recognition, 2018, pp. 7132–7141.
- [35] J. Park, S. Woo, J.-Y. Lee, and I. S. Kweon, "BAM: Bottleneck attention module," arXiv preprint arXiv:1807.06514, 2018.
- [36] S. Woo, J. Park, J.-Y. Lee, and I. So Kweon, "CBAM: Convolutional block attention module," in *Proceedings of the European Conference on Computer Vision*, 2018, pp. 3–19.
- [37] H. Zhao, J. Shi, X. Qi, X. Wang, and J. Jia, "Pyramid scene parsing network," in *Proceedings of the IEEE Conference on Computer Vision and Pattern Recognition*, 2017, pp. 2881–2890. 2, 4, 5, 6, 7
- [38] K. He, X. Zhang, S. Ren, and J. Sun, "Spatial pyramid pooling in deep convolutional networks for visual recognition," *IEEE Transactions on Pattern Analysis and Machine Intelligence*, vol. 37, no. 9, pp. 1904–1916, 2015.
- [39] L.-C. Chen, G. Papandreou, I. Kokkinos, K. Murphy, and A. L. Yuille, "Semantic image segmentation with deep convolutional nets and fully connected CRFs," arXiv preprint arXiv:1412.7062, 2014. 2, 4
- [40] L.-C. Chen, G. Papandreou, F. Schroff, and H. Adam, "Rethinking atrous convolution for semantic image segmentation," arXiv preprint arXiv:1706.05587, 2017. 2, 5, 6
- [41] L.-C. Chen, Y. Zhu, G. Papandreou, F. Schroff, and H. Adam, "Encoder-decoder with atrous separable convolution for semantic image segmentation," in *Proceedings of the European Conference on Computer Vision*, 2018, pp. 801–818.
- [42] J. Fu, J. Liu, H. Tian, Y. Li, Y. Bao, Z. Fang, and H. Lu, "Dual attention network for scene segmentation," in *Proceedings of the IEEE Conference* on Computer Vision and Pattern Recognition, 2019, pp. 3146–3154.
- [43] Y. Yuan, X. Chen, and J. Wang, "Object-contextual representations for semantic segmentation," arXiv preprint arXiv:1909.11065, 2020. 2, 7
- [44] X. Wang, R. Girshick, A. Gupta, and K. He, "Non-local neural networks," in *Proceedings of the IEEE Conference on Computer Vision* and Pattern Recognition, 2018, pp. 7794–7803. 2, 5
- [45] H. Zhang, K. Dana, J. Shi, Z. Zhang, X. Wang, A. Tyagi, and A. Agrawal, "Context encoding for semantic segmentation," in Proceedings of the IEEE Conference on Computer Vision and Pattern Recognition, 2018, pp. 7151–7160. 2, 4, 7
- [46] S. Liu, S. De Mello, J. Gu, G. Zhong, M.-H. Yang, and J. Kautz, "Learning affinity via spatial propagation networks," in *Proceedings of the Advances in Neural Information Processing Systems*, 2017, pp. 1520–1530.
- [47] X. Cheng, P. Wang, and R. Yang, "Depth estimation via affinity learned with convolutional spatial propagation network," in *Proceedings of the European Conference on Computer Vision*, 2018, pp. 103–119.
- [48] B. Zhou, H. Zhao, X. Puig, S. Fidler, A. Barriuso, and A. Torralba, "Scene parsing through ADE20K dataset," in *Proceedings of the IEEE Conference on Computer Vision and Pattern Recognition*, 2017, pp. 633–641.
- [49] F. Yu and V. Koltun, "Multi-scale context aggregation by dilated convolutions," arXiv preprint arXiv:1511.07122, 2015. 4
- [50] J. Fu, J. Liu, Y. Wang, Y. Li, Y. Bao, J. Tang, and H. Lu, "Adaptive context network for scene parsing," in *Proceedings of the IEEE Inter*national Conference on Computer Vision, 2019, pp. 6748–6757. 6, 7
- [51] C. Yu, J. Wang, C. Gao, G. Yu, C. Shen, and N. Sang, "Context prior for scene segmentation," in *Proceedings of the IEEE Conference on Computer Vision and Pattern Recognition*, 2020, pp. 12416–12425. 6,
- [52] H. Zhang, H. Zhang, C. Wang, and J. Xie, "Co-occurrent features in semantic segmentation," in *Proceedings of the IEEE Conference on Computer Vision and Pattern Recognition*, 2019, pp. 548–557.
- [53] H. Zhao, Y. Zhang, S. Liu, J. Shi, C. Change Loy, D. Lin, and J. Jia, "PSANet: Point-wise spatial attention network for scene parsing," in Proceedings of the European Conference on Computer Vision, 2018, pp. 267–283.
- [54] Z. Zhu, M. Xu, S. Bai, T. Huang, and X. Bai, "Asymmetric non-local neural networks for semantic segmentation," in *Proceedings of the IEEE International Conference on Computer Vision*, 2019, pp. 593–602. 7
- [55] J. He, Z. Deng, L. Zhou, Y. Wang, and Y. Qiao, "Adaptive pyramid context network for semantic segmentation," in *Proceedings of the IEEE Conference on Computer Vision and Pattern Recognition*, 2019, pp. 7519–7528.

- [56] J. Kopf, M. F. Cohen, D. Lischinski, and M. Uyttendaele, "Joint bilateral upsampling," ACM Transactions on Graphics, vol. 26, no. 3, pp. 96–es, 2007. 6
- [57] T.-W. Hui, C. C. Loy, and X. Tang, "Depth map super-resolution by deep multi-scale guidance," in *Proceedings of the European Conference* on Computer Vision, 2016, pp. 353–369. 7, 8
- [58] C. Guo, C. Li, J. Guo, R. Cong, H. Fu, and P. Han, "Hierarchical features driven residual learning for depth map super-resolution," *IEEE Transactions on Image Processing*, vol. 28, no. 5, pp. 2545–2557, 2018.
 7. 8
- [59] D. J. Butler, J. Wulff, G. B. Stanley, and M. J. Black, "A naturalistic open source movie for optical flow evaluation," in *Proceedings of the European Conference on Computer Vision*, 2012, pp. 611–625.
- [60] D. Scharstein and R. Szeliski, "A taxonomy and evaluation of dense two-frame stereo correspondence algorithms," *International Journal of Computer Vision*, vol. 47, no. 1-3, pp. 7–42, 2002.
- [61] Zuo et al., "Multi-scale frequency reconstruction for guided depth map super-resolution via deep residual network," *IEEE Transactions on Circuits and Systems for Video Technology*, vol. 30, no. 2, pp. 297–306, 2019. 7, 8
- [62] J. Park, H. Kim, Y.-W. Tai, M. S. Brown, and I. S. Kweon, "High-quality depth map upsampling and completion for RGB-D cameras," *IEEE Transactions on Image Processing*, vol. 23, no. 12, pp. 5559–5572, 2014. 8



Sung-Jea Ko (M'88-SM'97-F'12) received his Ph.D. degree in 1988 and his M.S. degree in 1986, both in Electrical and Computer Engineering, from State University of New York at Buffalo, and his B.S. degree in Electronic Engineering at Korea University in 1980. In 1992, he joined the Department of Electronic Engineering at Korea University where he is currently a Professor. From 1988 to 1992, he was an Assistant Professor in the Department of Electrical and Computer Engineering at the University of Michigan-Dearborn. He has published over 210

international journal articles. He also holds over 60 registered patents in fields such as video signal processing and computer vision.

Prof. Ko received the best paper award from the IEEE Asia Pacific Conference on Circuits and Systems (1996), the LG Research Award (1999), and both the technical achievement award (2012) and the Chester Sall award from the IEEE Consumer Electronics Society (2017). He was the President of the IEIE in 2013 and the Vice-President of the IEEE CE Society from 2013 to 2016. He is a member of the National Academy of Engineering of Korea. He is a member of the editorial board of the IEEE Transactions on Consumer Electronics



Min-Cheol Sagong received his B.S. degree in Electrical Engineering from Korea University in 2018. He is currently pursuing his Ph.D. degree in Electrical Engineering at Korea University. His research interests are in the areas of digital signal processing, computer vision, and artificial intelligence.



Yoon-Jae Yeo received his B.S. degree in Electrical Engineering from Korea University in 2017. He is currently pursuing his Ph.D. degree in Electrical Engineering at Korea University. His research interests are in the areas of image processing, computer vision, and deep learning.



Seung-Won Jung (S'06-M'11-SM'19) received the B.S. and Ph.D. degrees in electrical engineering from Korea University, Seoul, Korea, in 2005 and 2011, respectively. He was a Research Professor with the Research Institute of Information and Communication Technology, Korea University, from 2011 to 2012. He was a Research Scientist with the Samsung Advanced Institute of Technology, Yonginsi, Korea, from 2012 to 2014. He was an Assistant Professor at the Department of Multimedia Engineering, Dongguk University, Seoul, Korea, from

2014 to 2020. In 2020, he joined the Department of Electrical Engineering at Korea University, where he is currently an Associate Professor. He has published over 70 peer-reviewed articles in international journals. He received the Hae-Dong young scholar award from the Institute of Electronics and Information Engineers in 2019. His current research interests include image processing and computer vision.